

PCCP

Accepted Manuscript



This article can be cited before page numbers have been issued, to do this please use: Y. Yang, H. Wang, F. Liu, D. Yang, S. Bo, L. Qiu, Z. zhen and X. liu, *Phys. Chem. Chem. Phys.*, 2015, DOI:



This is an *Accepted Manuscript*, which has been through the Royal Society of Chemistry peer review process and has been accepted for publication.

Accepted Manuscripts are published online shortly after acceptance, before technical editing, formatting and proof reading. Using this free service, authors can make their results available to the community, in citable form, before we publish the edited article. We will replace this *Accepted Manuscript* with the edited and formatted *Advance Article* as soon as it is available.

You can find more information about *Accepted Manuscripts* in the [Information for Authors](#).

Please note that technical editing may introduce minor changes to the text and/or graphics, which may alter content. The journal's standard [Terms & Conditions](#) and the [Ethical guidelines](#) still apply. In no event shall the Royal Society of Chemistry be held responsible for any errors or omissions in this *Accepted Manuscript* or any consequences arising from the use of any information it contains.

ARTICLE

Synthesis of New Double-donor Chromophores with Excellent Electro-Optic Activity by Introducing Modified Bridges

Cite this: DOI: 10.1039/x0xx00000x

Received 00th December 2014,
Accepted 00th December 2014

DOI: 10.1039/x0xx00000x

www.rsc.org/

Yuhui Yang^{ab}, Haoran Wang^{ab}, Fenggang Liu^{ab}, Dan Yang^{ab}, Shuhui Bo^a, Ling Qiu^a, Zhen Zhen^a,
Xinhou Liu^{*a}

A series of chromophores y1-y3 based on the same bis(*N,N*-diethyl)aniline donor and tricyanofuran acceptor (TCF) linked together via the modified thiophene π -conjugation with different isolated groups have been synthesized and systematically investigated in this paper. Density functional theory (DFT) was used to calculate the HOMO–LUMO energy gaps and first-order hyperpolarizability (β) of these chromophores. Besides, to determine the redox properties of these chromophores, cyclic voltammetry (CV) experiments were performed. After introducing the isolation group into the thiophene, reduced energy gap of 1.03 and 1.02 eV were obtained for chromophore y2 and y3 respectively, much lower compared than chromophore y1 ($\Delta E = 1.13$ eV). These chromophores showed better thermal stability with their decomposition temperatures all above 220 °C. Besides, compared with results obtained from the chromophore (y1) without the isolated group, these new chromophores show better intramolecular charge-transfer (ICT) absorption. Most importantly, the high molecular hyperpolarizability (β) of these chromophores can be effectively translated into large electro-optic (EO) coefficients (r_{33}) in poled polymers. The electro-optic coefficient of poled films containing 25% wt of these new chromophores doped in amorphous polycarbonate (APC) afforded values of 149, 139 and 125 pm/V at 1310 nm for chromophores y1-y3 respectively. Besides, when the concentration was increased, film containing with chromophore y1 and y3 showed obvious phase separation, while film with chromophore y2 showed the maximum r_{33} values of 146 pm/V. Moreover, the electro-optic film prepared with these new chromophores gave greater stability. High r_{33} values indicated that the double donors of the bis(*N,N*-diethyl)aniline unit can efficiently improve the electron-donating ability and the isolated groups on the thiophene bridge can reduce intermolecular electrostatic interactions, thus enhancing the macroscopic EO activity. These properties, together with the good solubility, suggest the potential use of these new chromophores as advanced material devices.

1. Introduction

Integrated optical devices based on organic nonlinear optical (NLO) polymers have emerged as one of the enabling elements for a new generation of optical telecommunications, which needs fast modulation and switching of optical signals at the speed of 100 Gbit/s or above to accommodate anticipated growth in data traffic.¹⁻⁵ So the NLO materials have drawn considerable attention over the past two decades and have stimulated a research boom for materials with large EO activities, both at molecular level (β) and as processed materials (r_{33}).^{2, 5-7} An organic NLO material is generally composed of push-pull organic chromophores, in which a π -conjugated bridge is end-capped by a donor and an acceptor. In such molecules, the donor and acceptor substituents provide the requisite ground-state charge asymmetry, whereas the π -conjugation bridge provides a pathway for the ultrafast redistribution of electric charges under an applied external

electric field.^{4, 8, 9} Poled polymers are the most widely studied organic NLO materials. The macroscopic NLO response of such materials arises from the poling-induced polar order of noncentrosymmetric NLO chromophores in polymers.⁷ Unfortunately, in most of the poled polymers, the chromophore moieties which have a rod-like structure and the strong dipole-dipole interactions between chromophores have led to unfavorable antiparallel packing of the chromophores, making the conversion from the high β values of the chromophores to large macroscopic optical nonlinearities (r_{33}) a continual challenge.¹⁰⁻¹² So the most effective and facile way to improve the r_{33} values of the guest-host EO materials is the optimization of the push-pull chromophores.

To achieve higher EO activity and suppress the dipole interaction among chromophores, rational molecular designs of dipole chromophores have been made from the conjugated push-pull molecules. Many efforts have been carried out to

design and synthesize novel NLO chromophores, seeking to engineer NLO molecules both microscopically (β) and macroscopically (r_{33}).¹³⁻¹⁷ On one hand, structure-property relationships that have been established indicate that large β values of the chromophores can be achieved by careful modification of the strength of donor and acceptor moieties, as well as the nature of the π -conjugated spacer.^{18, 19} On the other hand, as reported, the introduction of some isolation groups (IG) to the chromophore moieties to further control the shape of the chromophore should be an efficient approach to minimize interactions between chromophores and thus enhance the poling efficiency.²⁰⁻²⁵

Based on the famous principle of site-isolation principle, as well as our previous work on the “double-donor chromophore”,^{5, 26, 27} we designed and synthesized three new double donor chromophores y1, y2 and y3. In our previous work, we have found that the double donors with two *N*, *N*-diethylaniline can improve the electron-donating ability thus enhance the optical nonlinearity. The one of the *N*, *N*-diethylaniline unit can act as both the additional donor and the isolation group (IG). On the other hand, The double donors chromophores having the double benzene rings with an appropriate angle make the special structure which is different from the general NLO chromophores showing the rod-like structure and can decrease the intermolecular electrostatic interactions. Thus it can enhance the macroscopic EO activity. In this paper, a new synthetic methodology of attaching two different substituents onto the π -conjugation bridge of NLO chromophore was developed to obtain two new NLO chromophores with adjustable shape, size and functionality on the side-chain. The motivation is to improve the EO activities of guest-host EO materials by a simple bridge-modifying method for NLO chromophores. Bridge modification was carried out to facilitate the chromophores with different steric hindrance and free mobility, which was expected to achieve the large macroscopic EO coefficients by optimizing the poling condition in guest-host EO polymers. In this paper, we designed and synthesized three double donor chromophores y1, y2 and y3 with different bridges. (Chart1). These chromophores showed great solubility in common organic solvents, better thermal stability (with their onset decomposition temperatures all above 220 °C), good compatibility with polymers, and large EO activity in the poled films. ¹H-NMR and ¹³C-NMR analysis were carried out to demonstrate the preparation of these chromophores. Thermal stability, photophysical properties and DFT calculations of these chromophores were systematically studied. Furthermore, the macroscopic EO activity (r_{33}) of these chromophores in amorphous polycarbonate were also analyzed.

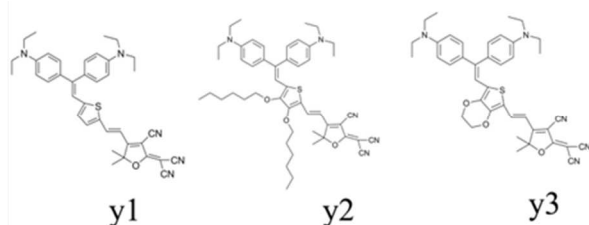
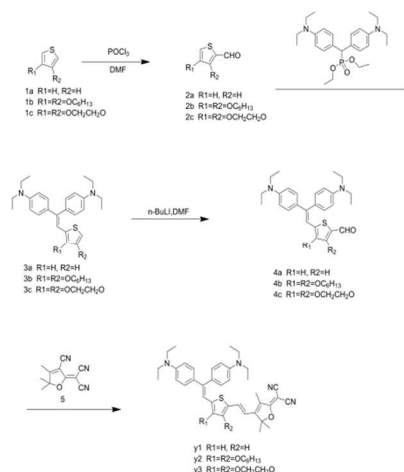


Chart1 The structures of chromophore y1-y3

2. Results and discussion.

2.1 synthesis and characterization of chromophores

The synthesis of chromophores y1, y2 and y3 are depicted in Schemes 1. These NLO chromophores were designed to have the same strong electron acceptor (TCF) and the same electron donor bis(*N,N*-diethyl)aniline group, but have different isolation groups on the thiophene π -conjugation. Chromophores y1, y2 and y3 were prepared starting from the phosphonate which was prepared using a procedure described in the literature.^{26, 28} Reacting phosphonate with different aldehyde (2a-2c) using sodium hydride as base under a Horner-Emmons reaction condition afforded (*E*)-alkene 3a-3c exclusively. Lithiation the (*E*)-alkene 3 with *n*-butyl lithium followed by the addition of DMF yielded the corresponding aldehyde 4a-4c. The target chromophores **y1** (with no substituent), **y2** (with two hexyloxy group) and **y3** (with cycloethoxy group) on the bridge thiophene ring were successfully obtained by condensing aldehydes 4a-4c with acceptor 5 (TCF) in ethanol in the presence of a catalytic amount of piperidine.



Scheme 1 Synthetic scheme for chromophore y1-y3

2.2 Thermal analysis

NLO chromophores must be thermally stable enough to withstand encountered high temperatures (>200 °C) in electric field poling and subsequent processing of chromophore/polymer materials. Thermal properties of these chromophores were measured by Thermogravimetric Analysis (TGA) with a heating rate of 10 °C·min⁻¹ under nitrogen. Fig. 1 shows the thermogravimetric analysis of chromophores y1, y2 and y3. All of the chromophores exhibited good thermal stabilities and their decomposition temperatures (T_d) were above 220 °C as summarized in Table 1. In particular, the highest T_d was observed for the chromophore y2 (259 °C), which indicated that the introduction of two hexyloxy groups on the thiophene ring is thermally robust. The excellent thermal stability of these chromophores makes them suitable for practical device fabrication and EO device preparation.

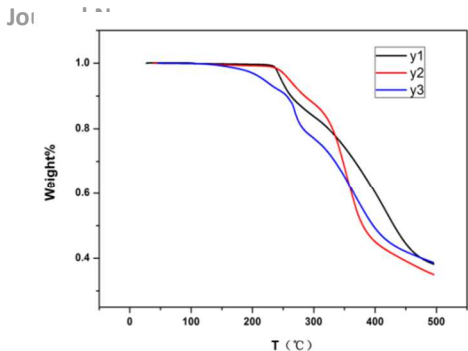


Figure 1 TGA curves of chromophores y1–y3 with a heating rate of 10 °C min^{−1} in a nitrogen atmosphere.

2.3 Optical properties

In order to reveal the effect of different isolated groups on the π -conjugation bridge on the intramolecular charge transfer (ICT) of dipolar chromophores, UV-Vis absorption spectra of three chromophores ($c = 1 \times 10^{-5}$ mol L^{−1}) were measured in a series of aprotic solvents with different polarity so that the solvatochromic behavior of the three chromophores could be investigated to explore the polarizability of chromophores in a wide range of dielectric environments (Fig. 2). The spectrum data are summarized in Table 1. The synthesized chromophores exhibited a similar π - π^* intramolecular charge-transfer (ICT) absorption band in the visible region. As shown in Fig. 2, in both non-polar and polar solvents such as 1,4-dioxane and CHCl₃, these chromophores exhibited a similar π - π^* intramolecular charge-transfer (ICT) absorption band with a continuous red-shift of the maximum absorption (λ_{max}) from y1 to y3. The peak wavelength of chromophores y3 showed a bathochromic shift of 66 nm from dioxane to chloroform, displaying a little larger solvatochromism compared with the chromophore y2 (61 nm in Table 1). The resulting spectrum data indicated that the chromophores y3 were more easily polarizable than chromophore y2.

Table1. Summary of Thermal and Optical Properties and EO Coefficients

of Chromophores y1-y3					
Chromophore	T _d ^a (°C)	λ_{max}^b (nm)	λ_{max}^c (nm)	$\Delta\lambda^d$ (nm)	r ₃₃ ^e (pm/V)
y1	249	725	654	71	149
y2	259	740	679	61	139
y3	221	753	687	66	125

^a T_d was determined by an onset point, and measured by TGA under nitrogen at a heating rate of 10 °C/min.

^b λ_{max} was measured in CHCl₃.

^c λ_{max} was measured in dioxane.

^d $\Delta\lambda = \lambda_{\text{max}}^b - \lambda_{\text{max}}^c$

^e r₃₃ values were measured at the wavelength of 1310nm.

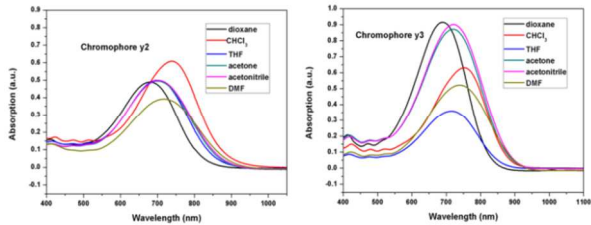


Figure 2 UV-Vis absorption spectra in different solvents of chromophore y2 and y3 ($c = 1 \times 10^{-5}$ mol L^{−1})

Traditional chromophores were easy to aggregate, which were beneficial for self-assembly. But it was unfavorable for NLO application, because the chromophores were easy to form the antiparallel aggregation. This phenomenon can be demonstrated by absorption intensity, wavelength and shape of absorption band in UV-vis spectra. To study the effect of these isolation groups on preventing chromophore aggregation, the absorption spectrum of these chromophores were measured in CHCl₃ at different concentration (from 0.005 mM to 0.07 mM). The Fig. 3 showed, the λ_{max} of the two chromophores at different concentration. As the concentration rose, no blue-shift or red-shift was found. Even at high concentration, no obvious characteristic absorption band of aggregation was observed. So we can confirm that there was no strong interaction among the chromophore molecules in solvents.

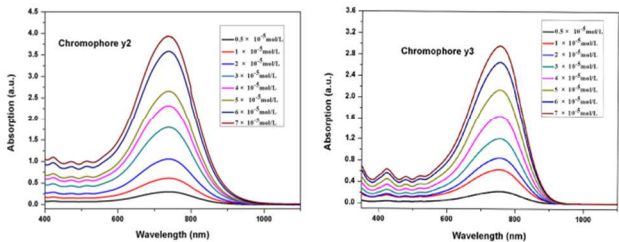


Figure 3 UV-Vis absorption spectra of different concentrations of chromophores y2 and y3 in CHCl₃

2.4 Theoretical calculations

In order to model the ground state molecular geometries, the HOMO–LUMO energy gaps and β values of these chromophores were calculated. The DFT calculations were carried out at the hybrid B3LYP level by employing the split valence 6-311 g** (d, p) basis set.^{29–31} The data obtained from DFT calculations are summarized in Table 2.

The frontier molecular orbitals are often used to characterize the chemical reactivity and kinetic stability of a molecule and to obtain qualitative information about the optical and electrical properties of molecules.^{31, 32, 33} Besides, the HOMO-LUMO energy gap is also used to understand the charge transfer interaction occurring in a chromophore molecule.^{33–35} In the case of these chromophores, Fig.4 represents the frontier molecular orbitals of chromophores y1-y3. According to Fig. 4, it is clear that the electronic distribution of the HOMO is delocalized over the thiophene linkage and benzene ring, whereas the LUMO is mainly constituted by the acceptor moieties.³³

Table2. Data from DFT calculations

Chromophores	E _{HOMO} / eV	E _{LUMO} / eV	ΔE^a / eV	ΔE^b / eV	β_{max}^c / 10 ^{−30} esu
y1	−5.04	−2.99	2.05	1.12	713
y2	−5.08	−3.09	1.99	1.03	652
y3	−5.05	−3.07	1.98	1.02	636

$\Delta E = E_{\text{LUMO}} - E_{\text{HOMO}}$.

^aResults was calculated by DFT

^bResults was from cyclic voltammetry experiment

^c β values were calculated using gaussian03at B3LYP/6-311 g** (d, p) level and the direction of the maximum value is transfer axis of the chromophores.

The HOMO and LUMO energy were calculated by DFT

calculations as shown in Table 2. The energy gap between the HOMO and LUMO energy for chromophores y1-y3 were 2.05 eV, 1.99 eV and 1.98 eV respectively. The HOMO-LUMO gap was the lowest for chromophore y3 (1.98 eV) and highest for chromophore y1 (2.05 eV). As reported,³³ the optical gap is lower and the charge-transfer (ICT) ability is greater, thus improving the nonlinearity. As a result, chromophore y2 and y3 showed the lower optical gap than chromophore y1, so it may indicate that chromophore y2 and y3 should exhibit better ICT and NLO properties than chromophore y1. This result corresponds with the UV-vis results.

Further, the theoretical microscopic Zero-frequency (static) molecular first hyperpolarizability (β) was calculated by Gaussian 03. As the reference reported earlier, the β has been calculated at the 6-311 g** (d, p) level in vacuum.³⁶ From this, the scalar quantity of β can be computed from the x, y, and z components according to the following equation:

$$\beta = (\beta_x^2 + \beta_y^2 + \beta_z^2)^{1/2} \quad (1)$$

$$\beta_i = \beta_{iii} + \frac{1}{3} \sum_{j \neq i} (\beta_{ijj} + \beta_{jii} + \beta_{jjj}), \quad i, j \in (x, y, z)$$

Where

The data obtained from DFT calculations were summarized in Table 2. There was no obvious change of the β values of these chromophores y1-y3 ($636 - 713 \times 10^{-30}$ esu), which illustrated that the substituent group on the thiophene bridge had little influence on their main conjugated structures under the simulated condition. This result is corresponded with the conclusion of UV-Vis spectra analysis.

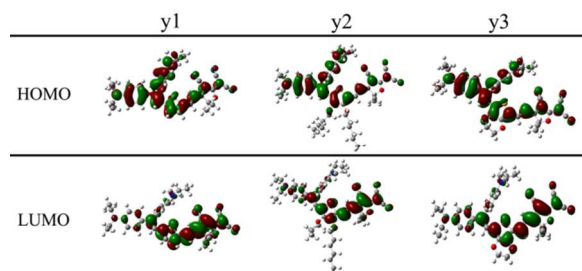


Figure 4 The frontier molecular orbitals of chromophores y1-y3

2.5 Electrochemical properties

To determine the redox properties of these chromophores, cyclic voltammetry (CV) experiments were performed on a CHI660D electrochemical workstation by a cyclic voltammetry (CV) technique in CH_3CN solution, using Pt disk electrode and a platinum wire as the working and counter electrodes, respectively, and a saturated Ag/AgCl electrode as the reference electrode in the presence of 0.1 M n-tetrabutylammoniumperchlorate as the supporting electrolyte. As shown in Fig. 5, chromophores y1, y2 and y3 all exhibited one quasi reversible oxidative wave with a half-wave potential, $E_{1/2} = 0.5(E_{\text{ox}} + E_{\text{red}})$, at about 0.55, 0.48 and 0.51 V respectively. Meanwhile, these chromophores had an irreversible reduction wave corresponding to the acceptor moieties at $E_{\text{red}} = -0.58, -0.55$ and -0.51 V (vs. Ag/AgCl). It showed an energy gap (ΔE) value of 1.13, 1.03 and 1.02 eV for chromophores y1, y2 and y3 respectively. The HOMO and LUMO levels of these new chromophores were calculated from their corresponding oxidation and reduction potentials. The HOMO levels of y1, y2 and y3 were estimated to be -4.95, -4.88 and -4.91 eV respectively. In the meantime, the

corresponding LUMO level of y1-y3 only showed slight changes at -3.82, -3.85 and -3.89 eV, respectively. This result corresponded with the conclusion of UV-Vis spectra analysis

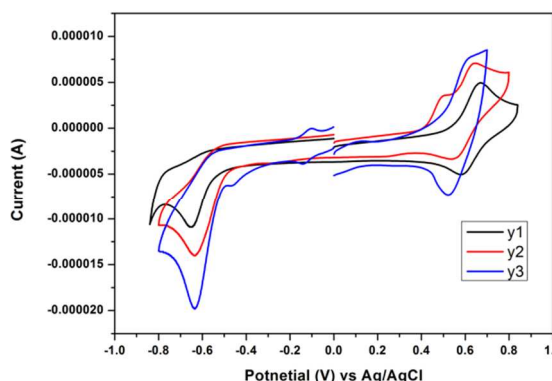


Figure 5 Cyclic voltammograms of chromophore y1-y3.

and the DFT results.

2.6 Electric field poling and EO property measurements

For studying EO property derived from these chromophores, a series of guest-host polymers were generated by formulating the chromophores into amorphous polycarbonate (APC) using dibromomethane as solvent. The resulting solutions were filtered through a 0.2 μm PTFE filter and spin-coated onto indium tin oxide (ITO) glass substrates. Films of doped polymers were baked in a vacuum oven at 80 $^{\circ}\text{C}$ overnight to ensure the removal of the residual solvent. The corona poling process was carried out at a temperature of 10 $^{\circ}\text{C}$ above the glass transition temperature (T_g) of the polymer. The r_{33} values were measured using the Teng-Man simple reflection technique at the wavelength of 1310 nm using a carefully selected thin ITO electrode with low reflectivity and good transparency in order to minimize the contribution from the multiple reflections.³⁷

The r_{33} values of films containing chromophores y1 (film-A), y2 (film-B), y3 (film-C) were measured in different loading densities, as shown in table 3 and Fig.6. For chromophore y1, the r_{33} values were gradually improved from 32 pm V^{-1} (10 wt%) to 149 pm V^{-1} (25 wt%), as the concentration of chromophores increased, the similar trend of enhancement was also observed for chromophore y2, whose r_{33} values increased from 37 pm V^{-1} (10 wt%) to 139 pm V^{-1} (25 wt%). Chromophore y3 gained the r_{33} value from 41 pm V^{-1} (10 wt%) to 125 pm V^{-1} (25 wt%).

Table 3 Summary of EO Coefficients of Chromophores y1-y3 at different densities

Wt%	r_{33} (pm/V)		
	y1	y2	y3
10	32	37	41
15	75	74	79
20	120	117	115
25	149	139	125
30	--	146	--
35	--	141	--

^a r_{33} values were measured at the wavelength of 1310nm.

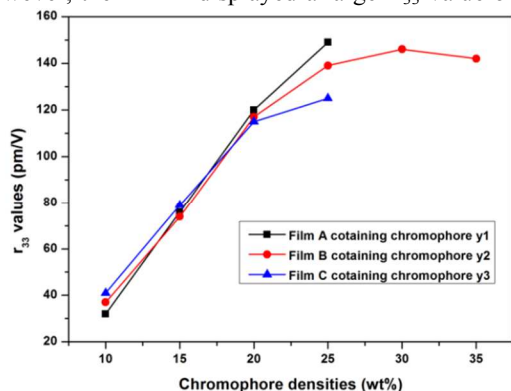
As reported earlier,²⁰ the introduction of some isolation groups into the chromophore moieties to further control the shape of the chromophore could be an efficient approach to minimize interactions between the chromophores. So by

introducing the isolation groups into the π -bridge, it controls the shape of the chromophore and decreased the interaction between the chromophore thus can increase the r_{33} value. But EO coefficient (r_{33}), defining the efficiency of translating molecular microscopic hyperpolarizability into macroscopic EO activities, was described as follows:

$$r_{33} = 2N f(\omega) \beta \langle \cos^3 \theta \rangle / n^4$$

where r_{33} is the EO coefficient of the poled polymer, N represents the aligned chromophore number density and $f(\omega)$ denotes the Lorentz-Onsager local field factors. The term $\langle \cos^3 \theta \rangle$ is the orientationally averaged acentric order parameter characterizing the degree of noncentrosymmetric alignment of the chromophore in the material and n represents the refractive index.⁵ Before poling, there is no EO activity in the EO material and the chromophores in material are thermal randomization. Electrical field induced poling was proceeded to induce the acentric ordering of chromophores. Realization of large electro-optic activity for dipolar organic chromophore-containing materials requires the simultaneous optimization of chromophore first hyperpolarizability (β), acentric order $\langle \cos^3 \theta \rangle$, and number density (N). But chromophores with large $\mu\beta$ generate intermolecular static electric field dipole-dipole interaction, which leads to the unfavorable antiparallel packing of chromophores, so that the number of truly oriented chromophore (N) is small. As a result, the isolation groups should be appropriate.

So it is not hard to explain the above r_{33} results. When the concentration of chromophore in APC is low, the intermolecular dipolar interactions are relatively weak and thus the influence of different isolated groups on r_{33} value is small. As the chromophore loading increased, the effect of inter-chromophore dipole-dipole is becoming stronger.^b Compared to chromophore y2, chromophore y3 with a better coplanar geometry presented a stronger negative effect of inter-chromophore dipole-dipole. So the film C containing chromophore y3 displayed a smaller r_{33} value than film B containing chromophore y2. Chromophore y2 with the two large isolated groups had the most effective steric hindrance. As shown in table 4, although the resulting r_{33} value of chromophore y2 was 139 pm/V, which was a little smaller than chromophore y1. When effectively normalizes the r_{33} value for the relative chromophore content, dividing the observed r_{33} by N yields a value of 7.52×10^{-19} pm cc/(V molecules), which is larger than chromophore y1 (6.07×10^{-19} pm cc/(V molecules)). Besides, chromophore y3 presented the smallest r_{33} values. Hence, film B containing chromophore y2 showed much higher efficiency of translating molecular microscopic hyperpolarizability into macroscopic EO activities. Besides, to our regret, as the loading density increasing from 25 wt % to 30 wt %, the film-A with the loading 30 wt % of y1 and film-C with the chromophore y3 presents an obvious phase separation. However, the film-B displayed a larger r_{33} value of 146 pm/V.



Th

Figure 6 EO coefficients of NLO thin films as a function of chromophore loading densities.

when the loading increased to 35%, film-B showed a downward trend. The enhancement of the EO activity further demonstrated that the isolated group on thiophene ring effectively suppressed the dipole-dipole interaction and assisted the orientation of chromophores during poling process. Meanwhile, as reported, the electrooptical features of organic materials principal role is important and begins to play the relation between the intra- and intermolecular dipole-dipole interaction and interaction with the phonon subsystem.^{38, 39}

Table 4 Representative r_{33} Values of the Chromophores.

Chromophores	y1	y2	y3
$r_{33}(\text{pm/V})^a$	149	139	125
N^b	2.455	1.849	2.239
r_{33}/N^c	6.07	7.52	5.59

^a Experimental value from simple reflection at 1310 nm.

^b Chromophore number density; in units of $\times 10^{20}$ molecules/cc.

^c r_{33} normalized by chromophore number density; in units of $\times 10^{-19}$ pm cc/(V molecules).

The stability of the poled EO films was also investigated. After annealing at 85°C for 100 h, the poled film of APC/25% chromophore y1, y2 and y3 poled APC/25% y1, y2 and y3 film could retain 78%, 81% and 76% (100h) of the initial values at 85°C respectively. This percentage was considerably higher enough.

Moreover, the order parameter changes of the poled EO films were studied through measuring the UV-Vis absorption spectra of EO films before and after poling. After the corona poling, the chromophores in the polymer were aligned, and the absorption intensity decreased due to birefringence. The order parameter (Φ) can be described according to the following equation: $\Phi = 1 - A_1/A_0$, where A_0 and A_1 are the absorbance of the un-poled and poled EO polymer films at normal incidence. The Φ values of poled APC/25%y1 film, APC/25%y2 film and APC/25% y3 film were about 22.3%, 20.6% and 15.1% respectively (Fig. 7), which showed that the Φ values had reached the average values and that the poling process was typically efficient. The Φ values are related to the chromophores' orientation, and more effective chromophore orientation would provide larger Φ values. The difference in the order parameter indicates that Films A/APC and B/APC have weaker inter-chromophore electrostatic interactions than Film-C/APC in high density. The obtained higher Φ values indicated that y1 and y2 could effectively orientate in the poled films. While, chromophore y3 with a better coplanar geometry presented a stronger negative effect of inter-chromophore dipole-dipole and showed the lowest Φ values. The high saturated loading density and larger r_{33} values of Films A and B were probably attributed to the fact that the chromophore structure isolated the chromophores from each other more effectively, thus improving the NLO effect at a higher chromophore loading density level. These results have a good agreement with the r_{33} values results.

These large r_{33} values and high stability together with our previous work of double donors chromophores can effectively prove that the double donor structure can really decrease the

interactions between the chromophores thus can increase the r_{33} value.

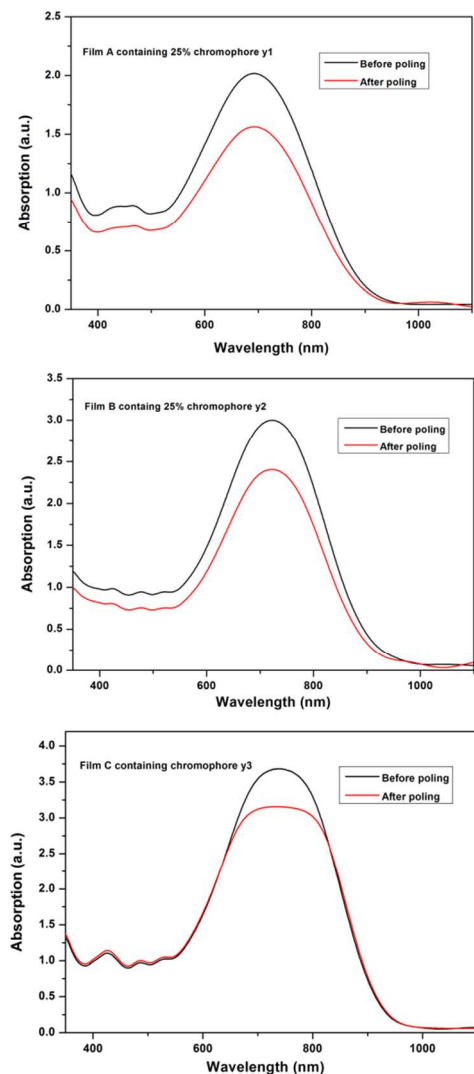


Figure 7 UV-Vis absorption spectra of E-O polymers before and after poling.

3. Experiments

3.1. Materials and instrumentation

^1H NMR spectra were determined by an Advance Bruker 400(400 MHz) NMR spectrometer (tetramethylsilane as internal reference). The MS spectra were obtained on MALDI-TOF-(Matrix Assisted Laser Desorption/Ionization of Flight) on BIFLEXIII(Broker Inc.) spectrometer. The UV-Vis spectra were performed on Cary 5000 photo spectrometer. The TGA was determined by TA5000-2950TGA (TA Co) with a heating rate of $10^\circ\text{C}/\text{min}$ under the protection of nitrogen. Cyclic voltammetry (CV) experiments were performed on a CHI660D electrochemical workstation by a cyclic voltammetry (CV) technique in CH_3CN solution, using Pt disk electrode and a platinum wire as the working and counter electrodes, respectively, and a saturated Ag/AgCl electrode as the reference electrode in the presence of 0.1 M *n*-tetrabutylammoniumperchlorate as the supporting electrolyte. The ferrocene/ferrocenium (Fc/Fc^+) couple was used as an internal reference. All chemicals, commercially available, are used without further purification unless stated. The DMF,

POCl_3 and THF were freshly distilled prior to its use. The 2-dicyanomethylene-3-cyano-4-methyl-2,5-dihydrofuran (TCF) acceptor was prepared according to the literature.⁴⁰

3.2. Synthesis

3.2.1 Synthesis of Chromophore y1

Chromophore y1 was synthesized according to the literature.²⁶

3.2.2 Synthesis of compound 2b

Dry DMF (3 mL) was dropwise added to 3 mL of phosphorus oxychloride (0.0327 mol) maintained at 0°C . After the solution was stirred for 15 min, compound 1b (7.78 g, 0.0274 mol) was added to the above Vilsmeier reagent, and the mixture was heated to 90°C for an additional 2 h. After cooling, the clear red solution was added dropwise to ice water with stirring, and the resulting mixture was allowed to stand for 2 h and extracted with CH_2Cl_2 (20 mL \times 3). The combined extracts were washed with water and dried over MgSO_4 . After filtration and removal of the solvent under vacuum, the crude product was purified by column chromatography to give a red liquid product (84%).

^1H NMR (400 MHz, CDCl_3) δ 9.99 (s, 1H), 6.62 (s, 1H), 4.32 (t, $J = 6.6$ Hz, 2H), 3.97 (t, $J = 6.6$ Hz, 2H), 1.85 – 1.69 (m, 4H), 1.52 – 1.39 (m, 4H), 1.37 – 1.30 (m, 8H), 0.94 – 0.85 (m, 6H).

^{13}C NMR (100 MHz, CDCl_3) δ 181.60, 153.33, 149.58, 124.31, 106.62, 73.76, 70.63, 31.45, 31.42, 29.90, 29.02, 25.69, 25.39, 22.52, 13.91.

MS (EI): m/z calcd for $\text{C}_{17}\text{H}_{28}\text{O}_3\text{S}$: 312.47; found: 312.49.

3.2.3 Synthesis of compound 3b

To a suspension of diethyl bis(4-(diethylamino) phenyl) methylphosphonate (1.5 g, 3.36 mmol), and 2b (936 mg, 3 mmol) in 20 mL dry THF and NaH (0.14 g, 5.6 mmol) were added and the mixture turned yellow. The mixture was stirred at room temperature for 24 h. Saturated NH_4Cl was added and the resulting mixture was extracted with EtOAc (20 mL \times 3). The combined extracts were washed with water and dried over MgSO_4 . After filtration and removal of the solvent under vacuum, the crude product was purified by column chromatography to give a yellow product (0.81 g, 44%).

^1H NMR (400 MHz, Acetone) δ 7.15 (m, 3H, overlap), 6.98 (d, $J = 8.6$ Hz, 2H), 6.77 (d, $J = 8.6$ Hz, 2H), 6.62 (d, $J = 8.9$ Hz, 2H), 6.04 (s, 1H), 4.07 (t, $J = 6.4$ Hz, 2H), 3.91 (t, $J = 6.4$ Hz, 2H), 3.48 – 3.35 (m, 8H), 1.81 – 1.69 (m, 4H), 1.64 – 1.42 (m, 4H), 1.38 – 1.23 (m, 8H), 1.21 – 1.11 (m, 12H), 0.90 (m, 6H).

MALDI-TOF: m/z calcd for $\text{C}_{38}\text{H}_{56}\text{N}_2\text{O}_2\text{S}$: 604.93 $[\text{M}]^+$; found: 604.87.

3.2.4 Synthesis of compound 4b

To a solution of 3a (1.21 g, 2.0 mmol) in dry THF (20 mL) was added a 2.4 M solution of *n*-BuLi in hexane (1.3 mL, 3.0 mmol) dropwise at -78°C under N_2 . After this mixture was stirred at this temperature for 1 h, and the dry DMF (0.20 mL, 2.4 mmol) was introduced. The resulting solution was stirred for another 1 h at -78°C and then allowed to warm up to room temperature. The reaction was quenched by water. THF was removed by evaporation. The residue was extracted with CH_2Cl_2 (3 \times 30 mL). The organic layer was dried (MgSO_4) and concentrated in vacuo. The residue was purified by column chromatography on silica gel (hexane/acetone, v/v, 10/1) to obtain a red solid (0.93 g, 74%).

^1H NMR (400 MHz, Acetone) δ 9.70 (s, 1H), 7.08 – 7.03 (m, 2H), 7.02 (s, 1H), 6.88 – 6.83 (m, 2H), 6.68 – 6.63 (m, 2H), 6.53 – 6.48 (m, 2H), 4.19 – 4.14 (m, 2H), 3.98 – 3.90 (m, 2H), 3.29 (m, 8H), 1.72 – 1.60 (m, 4H), 1.48 – 1.31 (m, 4H), 1.28 – 1.18 (m, 8H), 1.04 (m, 12H), 0.77 (m, 6H).

^{13}C NMR (100 MHz, Acetone) δ 179.72, 156.06, 148.25, 147.96, 146.26, 145.75, 137.31, 131.05, 128.97, 128.72, 125.07, 121.23, 112.14, 111.10, 110.93, 74.29, 74.22, 44.04, 44.01, 31.60, 31.40, 30.03, 29.80, 25.86, 25.40, 22.55, 22.39, 13.50, 13.42, 12.08, 12.00.

MALDI-TOF: m/z calcd for $\text{C}_{39}\text{H}_{56}\text{N}_2\text{O}_3\text{S}$: 632.94 $[\text{M}]^+$; found: 632.89.

3.2.5 Synthesis of chromophore y2

A mixture of aldehydic bridge 4b (0.632 g, 1 mmol) and acceptor 5 (0.24 g, 1.2 mmol) in ethanol (20 mL) in the presence of a catalytic amount of piperidine was stirred at 70 °C for 3 h. After removal of the solvent, the residue was purified by column chromatography on silica gel (hexane/ethyl acetate, v/v, 5:1), a dark solid was obtained (0.27 g, 33%).

^1H NMR (400 MHz, Acetone) δ 7.91 (d, J = 15.6 Hz, 1H), 7.30 – 7.25 (m, 2H), 7.25 (s, 1H), 7.00 (d, J = 8.6 Hz, 2H), 6.85 (d, J = 8.6 Hz, 2H), 6.69 (d, J = 9.0 Hz, 2H), 6.21 (d, J = 15.6 Hz, 1H), 4.32 (m, 2H), 4.10 (m, 2H), 3.46 (m, 8H), 1.88 – 1.76 (m, 4H), 1.73 (s, 6H), 1.54 (m, 4H), 1.42 – 1.31 (m, 8H), 1.27 – 1.13 (m, 12H), 0.91 (m, 6H).

^{13}C NMR (100 MHz, Acetone) δ 176.22, 172.76, 154.58, 148.20, 148.04, 147.82, 146.82, 139.35, 135.77, 131.60, 130.57, 129.27, 128.79, 120.15, 112.24, 111.57, 110.60, 110.36, 107.34, 96.31, 73.95, 73.43, 43.61, 43.53, 31.16, 30.77, 29.45, 25.17, 25.11, 25.01, 22.02, 21.86, 12.85, 11.57.

MALDI-TOF: m/z calcd for $\text{C}_{50}\text{H}_{66}\text{N}_5\text{O}_3\text{S}$: 814.13 $[\text{M}]^+$; found: 814.75.

3.2.6 Synthesis of compound 2c

In a similar manner described above, 2c was synthesized from 1c as yellow solid (92%).

^1H NMR (400 MHz, Acetone) δ 9.89 (d, J = 0.9 Hz, 1H), 7.03 (d, J = 0.9 Hz, 1H), 4.45 (dd, J = 5.2, 3.0 Hz, 2H), 4.34 (dd, J = 5.2, 3.0 Hz, 2H).

^{13}C NMR (100 MHz, Acetone) δ 179.92, 149.97, 143.11, 118.97, 110.96, 66.47, 65.37.

MS (EI): m/z calcd for $\text{C}_7\text{H}_6\text{O}_3\text{S}$: 170.19; found: 170.21.

3.2.7 Synthesis of compound 3c

In a similar manner described above, 3c was synthesized from 2c as yellow solid (74%).

^1H NMR (400 MHz, Acetone) δ 7.15 (d, J = 9.0 Hz, 2H), 7.05 (s, 1H), 7.00 (d, J = 8.7 Hz, 2H), 6.80 (d, J = 8.7 Hz, 2H), 6.65 (d, J = 9.0 Hz, 2H), 6.08 (s, 1H), 4.28 (m, 2H), 4.23 – 4.18 (m, 2H), 3.44 (m, 8H), 1.19 (m, 12H).

^{13}C NMR (100 MHz, Acetone) δ 147.84, 147.21, 141.40, 139.56, 138.63, 131.42, 130.22, 127.78, 126.48, 117.45, 112.27, 111.66, 111.51, 98.11, 64.90, 64.62, 44.07, 12.13, 12.08.

MALDI-TOF: m/z calcd for $\text{C}_{28}\text{H}_{34}\text{N}_2\text{O}_2\text{S}$: 462.65 $[\text{M}]^+$; found: 462.61.

3.2.8 Synthesis of compound 4c

In a similar manner described above, 4c was synthesized from 3c as red solid (83%).

^1H NMR (400 MHz, CDCl_3) δ 9.70 (s, 1H), 7.24 (d, J = 8.8 Hz, 2H), 7.06 (s, 1H), 7.03 (d, J = 8.6 Hz, 2H), 6.72 (d, J = 8.6 Hz, 2H), 6.58 (d, J = 8.8 Hz, 2H), 4.33 (m, 2H), 4.31 (m, 2H), 3.46 – 3.32 (m, 8H), 1.19 (m, 12H).

^{13}C NMR (100 MHz, CDCl_3) δ 178.26, 147.30, 146.89, 146.73, 144.66, 137.61, 130.14, 129.37, 128.15, 127.97, 123.94, 114.25, 111.20, 110.02, 109.37, 64.41, 63.52, 43.37, 43.33, 11.62.

MALDI-TOF: m/z calcd for $\text{C}_{29}\text{H}_{34}\text{N}_2\text{O}_3\text{S}$: 490.66 $[\text{M}]^+$; found: 491.19.

3.2.9 Synthesis of chromophore y3

In a similar manner described above, chromophore y3 was synthesized from 4c and acceptor 5, as a dark solid (40%).

^1H NMR (400 MHz, Acetone) δ 7.64 (d, J = 15.1 Hz, 1H), 7.13 (d, J = 9.0 Hz, 2H), 7.04 (s, 1H), 6.89 (d, J = 8.7 Hz, 2H), 6.73 (d, J = 8.7 Hz, 2H), 6.57 (d, J = 9.0 Hz, 2H), 6.18 (d, J = 15.1 Hz, 1H), 4.39 (m, 2H), 4.32 (m, 2H), 3.41 – 3.28 (m, 8H), 1.60 (s, 6H), 1.08 (m, 12H).

^{13}C NMR (100 MHz, Acetone) δ 184.70, 176.72, 111.69, 111.08, 109.54, 104.58, 100.89, 97.14, 62.11, 62.04, 56.48, 43.39, 43.34, 27.07, 25.87, 25.11, 25.03, 23.33, 16.15, 16.10, 11.51.

MALDI-TOF: m/z calcd for $\text{C}_{40}\text{H}_{41}\text{N}_5\text{O}_3\text{S}$: 671.85 $[\text{M}]^+$; found: 672.12.

Conclusions

In this research, a series of NLO chromophores based on thiophene bridge bearing on different substituted groups with the same bis(*N,N*-diethylaniline) donors and electron acceptor (TCF) have been synthesized and systematically investigated by NMR, MS and UV-vis absorption spectra. The energy gap between ground state and excited state together with molecular nonlinearity were studied by UV-vis absorption spectroscopy, DFT calculations and CV measurements. Theoretical and experimental investigations suggest that the isolation group play a critical role in affecting the linear and nonlinear properties of dipolar chromophores. In general, the energy gap of y2 and y3 chromophore is 1.03 and 1.02 eV respectively, which is much lower than y1 chromophore without isolation group on thiophene ring. These results confirmed that chromophores with double donors and with different isolation groups on the thiophene bridge exhibiting good thermal stability and large molecular hyperpolarizabilities, which can be effectively translated into very large EO coefficients in poled polymers. The poling results of guest-host EO polymers with 25 wt% of these chromophores showed that polymers with chromophores y1- y3 afforded the large r_{33} values of 149, 139 and 125 pm/V respectively. Moreover, the stability of poled APC/25% y1, y2 and y3 film could retain 78%, 81% and 76% (100h) of the initial values at 85 °C respectively. Those consequences indicate that these chromophores with double *N,N*-diethylaniline donors and isolated groups on the thiophene bridge could efficiently reduce the interchromophore electrostatic interactions and enhance the macroscopic optical nonlinearity. These novel chromophores showed promising applications in NLO chromophore synthesis. We believe that these novel chromophores can be used in exploring high-performance organic EO and photorefractive materials where both thermal stability and optical nonlinearity are of equal importance.

Acknowledgements

We are grateful to the National Nature Science Foundation of China (no. 61101054) for financial support.

Notes and references

^a Key Laboratory of Photochemical Conversion and Optoelectronic Materials, Technical Institute of Physics and

Chemistry, Chinese Academy of Sciences, Beijing 100190, PR China

^b University of Chinese Academy of Sciences, Beijing 100043, PR China

* Corresponding authors. Tel.: +86-01-82543528; Fax: +86-01-62554670.

E-mail address: xinhoulia@foxmail.com and xhliu@mail.lpc.ac.cn (X. Liu)

1. J. Luo, Y.-J. Cheng, T.-D. Kim, S. Hau, S.-H. Jang, Z. Shi, X.-H. Zhou and A. K. Y. Jen, *Org. Lett.*, 2006, **8**, 1387-1390.
2. Y. Q. Shi, C. Zhang, H. Zhang, J. H. Bechtel, L. R. Dalton, B. H. Robinson and W. H. Steier, *Science*, 2000, **288**, 119-122.
3. S.-K. Kim, Y.-C. Hung, B.-J. Seo, K. Geary, W. Yuan, B. Bortnik, H. R. Fetterman, C. Wang, W. H. Steier and C. Zhang, *Appl. Phys. Lett.*, 2005, **87**, 061112.
4. L. R. Dalton, P. A. Sullivan and D. H. Bale, *Chem. Rev.*, 2010, **110**, 25-55.
5. L. R. Dalton, D. Lao, B. C. Olbright, S. Benight, D. H. Bale, J. A. Davies, T. Ewy, S. R. Hammond and P. A. Sullivan, *Opt. Mater.*, 2010, **32**, 658-668.
6. P. A. Sullivan and L. R. Dalton, *Acc. Chem. Res.*, 2010, **43**, 10-18.
7. S. R. Marder, B. Kippelen, A. K. Y. Jen and N. Peyghambarian, *Nature*, 1997, **388**, 845-851.
8. X. Zhang, I. Aoki, X. Piao, S. Inoue, H. Tazawa, S. Yokoyama and A. Otomo, *Tetrahedron Lett.*, 2010, **51**, 5873-5876.
9. L. R. Dalton, *Thin Solid Films*, 2009, **518**, 428-431.
10. L. R. Dalton, A. W. Harper and B. H. Robinson, *Proceedings of the National Academy of Sciences of the United States of America*, 1997, **94**, 4842-4847.
11. D. Yu, A. Gharavi and L. Yu, *J. Am. Chem. Soc.*, 1995, **117**, 11680-11686.
12. M. J. Cho, S. K. Lee, J. I. Jin, D. H. Choi and L. R. Dalton, *Thin Solid Films*, 2006, **515**, 2303-2309.
13. Y. J. Cheng, J. D. Luo, S. Hau, D. H. Bale, T. D. Kim, Z. W. Shi, D. B. Lao, N. M. Tucker, Y. Q. Tian, L. R. Dalton, P. J. Reid and A. K. Y. Jen, *Chem. Mater.*, 2007, **19**, 1154-1163.
14. J. Wu, J. Liu, T. Zhou, S. Bo, L. Qiu, Z. Zhen and X. Liu, *RSC Advances*, 2012, **2**, 1416.
15. J. Wu, C. Peng, H. Xiao, S. Bo, L. Qiu, Z. Zhen and X. Liu, *Dyes and Pigments*, 2014, **104**, 15-23.
16. S. R. Hammond, O. Clot, K. A. Firestone, D. H. Bale, D. Lao, M. Haller, G. D. Phelan, B. Carlson, A. K. Y. Jen, P. J. Reid and L. R. Dalton, *Chem. Mater.*, 2008, **20**, 3425-3434.
17. M. He, T. M. Leslie, J. A. Sinicropi, S. M. Garner and L. D. Reed, *Chem. Mater.*, 2002, **14**, 4669-4675.
18. R. Andreu, M. J. Blesa, L. Carrasquer, J. Garín, J. Orduna, B. Villacampa, R. Alcalá, J. Casado, M. C. Ruiz Delgado, J. T. López Navarrete and M. Allain, *J. Am. Chem. Soc.*, 2005, **127**, 8835-8845.
19. X.-H. Zhou, J. Luo, J. A. Davies, S. Huang and A. K. Y. Jen, *J. Mater. Chem.*, 2012, **22**, 16390-16398.
20. W. B. Wu, J. G. Qin and Z. Li, *Polymer*, 2013, **54**, 4351-4382.
21. Z. Li, Q. Q. Li and J. G. Qin, *Polymer Chemistry*, 2011, **2**, 2723-2740.
22. W. B. Wu, Q. Huang, G. F. Qiu, C. Ye, J. G. Qin and Z. Li, *J. Mater. Chem.*, 2012, **22**, 18486-18495.
23. W. Wu, R. Tang, Q. Li and Z. Li, *Chem. Soc. Rev.*, 2015, DOI: 10.1039/C4CS00224E.
24. W. B. Wu, C. Wang, R. L. Tang, Y. J. Fu, C. Ye, J. G. Qin and Z. Li, *Journal of Materials Chemistry C*, 2013, **1**, 717-728.
25. Z. a. Li, Z. Li, C. a. Di, Z. Zhu, Q. Li, Q. Zeng, K. Zhang, Y. Liu, C. Ye and J. Qin, *Macromolecules*, 2006, **39**, 6951-6961.
26. Y. Yang, H. Xu, F. Liu, H. Wang, G. Deng, P. Si, H. Huang, S. Bo, J. Liu, L. Qiu, Z. Zhen and X. Liu, *Journal of Materials Chemistry C*, 2014, **2**, 5124-5132.
27. L. Dalton and S. Benight, *Polymers*, 2011, **3**, 1325-1351.
28. S. Zheng, S. Barlow, T. C. Parker and S. R. Marder, *Tetrahedron Lett.*, 2003, **44**, 7989-7992.
29. R. M. Dickson and A. D. Becke, *J. Chem. Phys.*, 1993, **99**, 3898-3905.
30. M. Frisch, G. Trucks, H. Schlegel, G. Scuseria, M. Robb, J. Cheeseman, J. Montgomery Jr, T. Vreven, K. Kudin and J. Burant, *Gaussian Inc., Pittsburgh, PA*, 2003.
31. C. Lee and R. G. Parr, *Physical Review A*, 1990, **42**, 193-200.
32. X. Ma, F. Ma, Z. Zhao, N. Song and J. Zhang, *J. Mater. Chem.*, 2010, **20**, 2369.
33. R. V. Solomon, P. Veerapandian, S. A. Vedha and P. Venuvanalingam, *J. Phys. Chem. A*, 2012, **116**, 4667-4677.
34. R. M. El-Shishtawy, F. Borbone, Z. M. Al-Amshany, A. Tuzi, A. Barsella, A. M. Asiri and A. Roviello, *Dyes and Pigments*, 2013, **96**, 45-51.
35. J. Y. Wu, J. L. Liu, T. T. Zhou, S. H. Bo, L. Qiu, Z. Zhen and X. H. Liu, *Rsc Advances*, 2012, **2**, 1416-1423.
36. K. S. Thanthiriwatte and K. M. N. de Silva, *Journal of Molecular Structure-Theochem*, 2002, **617**, 169-175.
37. C. C. Teng and H. T. Man, *Appl. Phys. Lett.*, 1990, **56**, 1734.
38. I. Fuks-Janczarek, I. V. Kityk, R. Miedzinski, E. Gondek, J. Ebothe, L. Nzoghe-Mendome and A. Danel, *Journal of Materials Science-Materials in Electronics*, 2007, **18**, 519-526.
39. I. Fuks-Janczarek, R. Miedzinski, E. Gondek, P. Szlachcic and I. V. Kityk, *Journal of Materials Science-Materials in Electronics*, 2008, **19**, 434-441.
40. M. Q. He, T. M. Leslie and J. A. Sinicropi, *Chem. Mater.*, 2002, **14**, 2393-2400.

Graphical Absrtact

New double-donor chromophores were synthesized and the large hyperpolarizability can be effectively translated into large electro-optic coefficients.

